PART I

INSTRUMENTATION – MEASUREMENT OF MAGNETIC FIELDS IN THE SOLAR ATMOSPHERE

https://doi.org/10.1017/S0074180900022336 Published online by Cambridge University Press

THE MEASUREMENT OF SOLAR MAGNETIC FIELDS

JACQUES M. BECKERS

Sacramento Peak Observatory, Air Force Cambridge Research Laboratories, Sunspot, New Mexico 88349, U.S.A.

Abstract. The different methods which have been used, or which may be used in the future, to measure solar magnetic fields are described and discussed. Roughly these can be divided into three groups (a) those which use the influence of the magnetic field on the electromagnetic radiation, (b) those which use the influence of the field on the structure of the solar atmosphere (MHD effects), and (c) those which use theoretical arguments. The former include the Zeeman effect, the Hanle effect, the gyro and synchrotron radiations and the Faraday rotation of radiowaves. The second includes the alignment of details at all levels of the solar atmosphere, and the calcium network, and the third makes use, for example, of the assumption of equipartition between magnetic and kinetic energy density.

1. Introduction

In preparing this discussion of the methods used to measure solar magnetic fields, I was tempted to describe in detail the refinements used today in the measurement of the field by means of the Zeeman effect. Other papers on this topic do, however, already exist and it seemed therefore wasteful. I, therefore, decided to try to review and discuss all the known different ways of magnetic field determination on the Sun.

I will divide these ways into three groups. The first utilizes the influence of the magnetic field on the solar electromagnetic radiation. It includes measurements made by means of the Zeeman effect, the Hanle effect (or resonance scattering), the gyro-resonance radiation and synchrotron radiation in the radio region, and the Faraday rotation of radio waves. The second group makes use of the influence of the magnetic field on the temperature and density structure of the solar atmosphere. In it fall the relation of the field with the Hα fibril structure and the calcium emission network. The third group utilizes theoretical arguments for the magnetic field determination. It includes, for example, the potential field calculations of coronal magnetic fields, and the equipartition of magnetic and kinetic energy.

2. Magnetic Fields as Determined by their Influence on Electromagnetic Radiation

2.1. The Zeeman Effect

Solar Magnetographs utilizing the Zeeman effect have been described by Zhulin *et al.* (1962), Evans (1966), Beckers (1968b), and others. The Zeeman effect refers to the splitting of spectral lines in the presence of a magnetic field. For not too strong fields, where the Paschen-Back effect is negligible (and this is the case for all lines, but the Lithium lines, for magnetic field strengths encountered on the Sun), this splitting is proportional to the field strength. The splitting pattern is dependent on the details of the atomic transition (Beckers 1969); the strengths and the polarization of the components is dependent on the direction of the magnetic field. For strong fields

Howard (ed.), Solar Magnetic Fields, 3–23.

($B > 2000$ G) and for favorable lines (Zeeman triplets, $g = 3$) the splitting is large enough to be directly measurable. In that case, it is rather simple to measure both the amount and the direction of the magnetic field (see e.g. Beckers and Schröter (1969)). Most magnetographs are, however, built to measure very weak fields for which the Zeeman splitting $\Delta\lambda_B$ is much smaller than the line width. In this case, the splitting manifests itself only in a polarization of the line profile. The relation between this polarization and the magnetic field will be discussed in detail in Dr. Stenflo's review article. It is sufficient for the present discussion to give an approximate expression for this polarization based on the Seares formulae (Seares (1913)). One easily derives the following four Stokes parameters:

$$I = \text{Intensity} = \tfrac{1}{4}(1 + \cos^2\gamma)\,[p(\lambda - \Delta\lambda_B) + p(\lambda + \Delta\lambda_B)] + \tfrac{1}{2}\sin^2\gamma\, p(\lambda) \tag{1}$$

$$Q = \text{Linear polarization} = \tfrac{1}{4}\sin^2\gamma\,[2p(\lambda) - p(\lambda + \Delta\lambda_B)] \tag{1'}$$

$$U = 0 \tag{1''}$$

$$V = \text{Circular polarization} = \tfrac{1}{2}\cos\gamma\,[p(\lambda + \Delta\lambda_B) - p(\lambda - \Delta\lambda_B)]. \tag{1'''}$$

In Equations (1) the azimuth of the magnetic field coincides with the reference direction for the Q-Stokes parameter, $p(\lambda)$ = line profile and γ = angle between **B** and the line of sight. For small $\Delta\lambda_B$ a Taylor expansion of (1) gives:

$$I \approx p(\lambda) \tag{2}$$

$$Q \approx -0.25\,\Delta\lambda_B^2 \sin^2\gamma\, \mathrm{d}^2p/\mathrm{d}\lambda^2 \qquad (:)\ B_\perp^2 \tag{2'}$$

$$U \approx 0 \tag{2''}$$

$$V \approx \Delta\lambda_B \cos\gamma\, \mathrm{d}p/\mathrm{d}\lambda \qquad (:)\ B_\parallel . \tag{2'''}$$

By measuring V one therefore can determine the longitudinal magnetic field $B_\parallel$ and by measuring the direction and the amount Q of linear polarization one can measure the square of the transverse field $B_\perp^2$. Because for weak fields $Q \ll V$ it is very hard to measure transverse fields. Zeeman magnetographs are in fact polarimeters which measure either V (Longitudinal Magnetographs) or V, Q and U (Vector Magnetographs) and which through some kind of calibration procedure interpret these in terms of $B_\parallel$ and $B_\perp$ and through these in **B**. The measurement of the polarization is generally done by means of electro-optical light modulators combined with polarizers and retardation plates. The number of possible combinations of these is virtually inexhaustible as the compilation of existing magnetographs in Table I shows. Those instruments in Table I which are built specifically to measure magnetic fields are called magnetographs. The two polarimeters are general purpose instruments which among others can measure the polarization due to the Zeeman effect. Figure 1 shows the optical diagram of the HAO polarimeter which is presently under construction. The two electro-optical light modulators cause the light intensity to vary with certain frequencies, each of the four Stokes parameters I, Q, U and V being connected with the amplitude of a specific frequency. This particular instrument will be connected with a

TABLE I

Summary of Zeeman magnetographs

Location	Type*	Lay-out**	Reference(s)
Aerospace	*L*	Photographic by image subtraction	–
Aerospace	*L*	Video system (under construction)	–
Cambridge (Malta)	*L*	EOLM (λ/4,45°), *P*	Beggs *et al.* (1964)
Capri	*V*	λ/4 (rot), EOLM (λ/4,45°), *P*	Deubner *et al.* (1969)
Crimea	*V*	λ/4 (0° and 45°), EOLM (λ/4,45°), *P*	Stepanov *et al.* (1962)
Hawaii	*P*	λ/4 (rot), *P*	–
HAO	*L*	EOLM (λ/4,45°), *P* (automatic calibration)	Lee *et al.* (1965)
HAO	*P*	EOLM (λ/2.61,0°), EOLM (λ/6.50,45°), λ/4 (45°), *P* (under construction)	–
Huntsville	*V*	Video System (under construction)	–
Izmiran	*V*	λ/4 (15°), EOLM (λ/4,45°), *P*	Ioshpa *et al.* (1962, 1965)
Kitt Peak	*V*	{λ/2 (22.5°) and none}, EOLM (λ/2,45°), *P*	Livingston *et al.* (1970)
Kitt Peak	*L*	EOLM (λ/4,45°), *P* (40 channel)	Livingston *et al.* (1970)
Kodaikanal	*L*	EOLM (λ/4,45°), *P*	
Locarno	*V*	λ/13.7 (0°), EOLM (λ/4,45°), *P*	Wiehr (1969)
Meudon	*V*	Photographic with lambdameter	Rayrole (1967)
Mt. Wilson	*L*	EOLM (λ/4,45°), *P*	Babcock (1953)
Ondrejov	*V*	λ/4 (13°), λ/4 (45°), EOLM (λ/4,45°), *P*	Kuznetzov *et al.* (1966)
Pulkovo	*V*	λ/2 (rot), EOLM (λ/4,45°), *P*	–
Rome	*L*	EOLM (λ/4,45°), *P*	–
Sac Peak	*L*	λ/4 (45°), *P* (measures spectrum separation)	Evans (1966)
Sibizmir	*V*	λ/4 (13°), λ/4 (45°), EOLM (λ/4,45°), *P*	Kuznetzov *et al.* (1966)
Sydney	*L*	Video System (under construction)	–

* *L* = Longitudinal Magnetograph, *V* = Vector Magnetograph, *P* = Polarimeter.
Most vector magnetographs work also in longitudinal mode only.
** Explanation: λ/4 (20°) = quarter wave plate with optical axis at 20° with respect to the axis of polarizer *P*.
EOLM (λ/4,45°) = Electro-optical light modulator, modulated at $\pm$ λ/4 axis makes 45° with *P*.

rapidly scanning spectrometer so that the line profile can be measured in all Stokes parameters.

The Zeeman magnetograph is the best instrument so far to measure solar fields. There are, however, a number of serious difficulties in deriving the magnetic field from the magnetograph signal. I want to discuss these shortly.

(a) The calibration of the polarization in terms of $B_{\parallel}$ or $B_{\perp}$ is often very difficult. Partly this is due to a variation of the quantities $\mathrm{d}p/\mathrm{d}\lambda$ and $\mathrm{d}^2p/\mathrm{d}\lambda^2$ across the solar surface partly this is due to as yet poorly understood differences between calibration curves which are derived in different ways (Deubner (1969), Severny (1967)). Some longitudinal magnetographs solved much of these problems by either measuring the

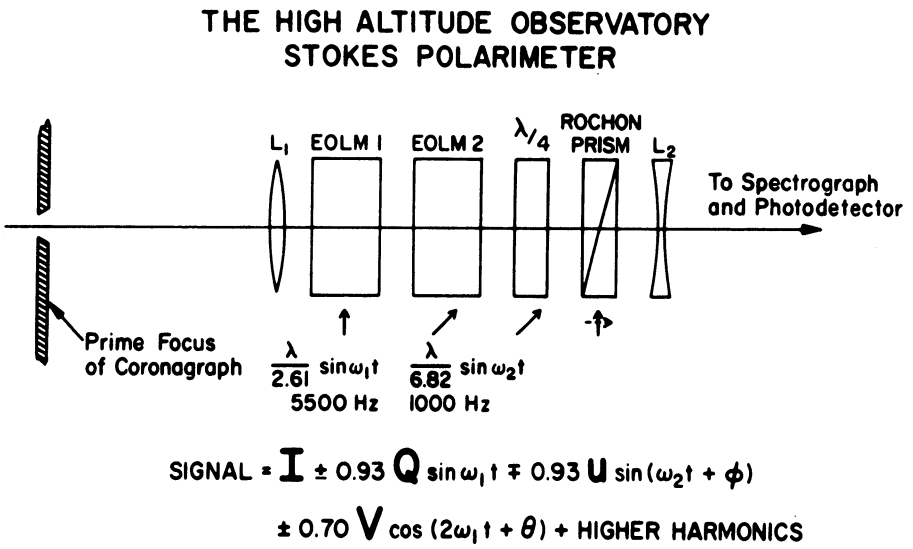

Fig. 1. Diagram of the HAO polarimeter. The polarimeter is mounted in the prime focus of the 40 cm coronograph before any reflections take place. EOLM 1 and 2 are two *KD*P* electro-optical light modulators and $\lambda/4$ is an achromatic quarter wave plate.

$dp/d\lambda$ (HAO magnetograph) or by measuring the difference in position of the line profiles as seen in opposite circular polarizations (Sac Peak magnetograph).

(b) In some vector magnetographs the Q and V Stokes parameters are detected at the same frequency. They are separated by respectively adding and subtracting the blue and red wing signals since presumably $dp/d\lambda$ (Equations (2)) is opposite in sign in the two wings whereas $d^2p/d\lambda^2$ is equal in sign. There is, however, no reason that the $dp/d\lambda$ is also equal in amplitude since asymmetric line profiles are quite common on the Sun so that this addition and subtraction may not separate the circular and linear polarization thus creating the danger of a serious mixing of the signals.

(c) The horizontal fine structure of the magnetic fields can influence strongly the measurements. One measures for example in a longitudinal magnetograph the circular polarization averaged over the scanning aperture or

$$V = \langle V(x, y) \rangle = \left\langle \Delta\lambda_B \cos\gamma \frac{dp}{d\lambda} I_{\text{cont}} \right\rangle . \tag{3}$$

One therefore measures the average field across the aperture only if the product $dp/d\lambda \cdot I_{\text{cont}}$ is constant. Generally, this is not the case however. This is believed to be the principle cause for the large differences (as much as a factor of 3) in the magnetic field measurements made in different lines as shown in Figure 2. Similarly one also only measures the average of the square of the transverse field $B_\perp^2$ if $d^2p/d\lambda^2 \cdot I_{\text{cont}}$ is constant. Even if one eventually manages to measure the proper averages $\langle B_\parallel \rangle$ and $\langle B_\perp^2 \rangle$ one does not know yet the average vector field strength and direction because the averaging of the transverse field is done over the second power. One can measure,

https://doi.org/10.1017/S0074180900022336 Published online by Cambridge University Press

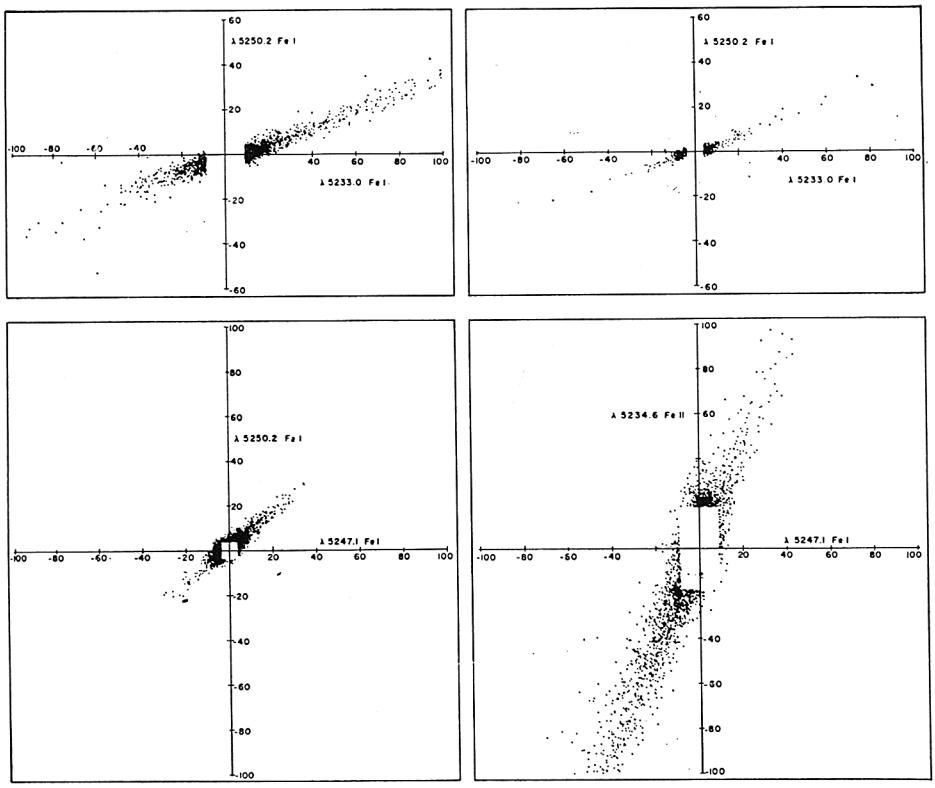

Fig. 2. Comparison of the longitudinal magnetic field as measured in different lines by Harvey and Livingston (1969).

for example, the wrong direction of the magnetic field vector even if this direction is constant across the aperture and only the field amplitude changes.

(d) Vertical variations of the magnetic field cause other problems especially in strong lines like Hα which are formed over a large range in depth over which these variations may be very large. One may in these lines measure magnetic fields which are very different in size and even opposite in sign, as compared to the real fields (similar effects for Doppler shifts have been discussed by Athay (1970) and Beckers (1968a)). In addition, one has to consider in this case magneto-optical effects like Faraday rotation as will be discussed by Dr. Stenflo.

These difficulties in the interpretation of the magnetograph signals have fortunately not withheld people from measuring solar fields. I mention them only to warn against relying too strongly on the quantitative values of the field. For weak fields deviations of 50% and more could easily occur.

Recent developments in solar magnetographs include adaptation of digital techniques, as well as computer reduction and visual display. Figure 3 shows for example an isogauss map derived by computer from the Sac Peak magnetometer signal. Figure 4 shows an example of the Kitt Peak vector magnetograph results. Instead of drawing

https://doi.org/10.1017/S0074180900022336 Published online by Cambridge University Press

isogauss lines this form of display generates an intensity picture for the signals of interest. The same is done for the full solar disk longitudinal field measurements made with the 40 channel magnetometer at Kitt Peak as displayed in Figure 5. Only by using simultaneous measurements in 40 channels does the photoelectric magnetograph compare in sensitivity with photographic ways measuring magnetic field (Beckers, 1968b). Figure 6 shows a magnetogram obtained at the Aerospace Observatory by direct photographic subtraction of images photographed in opposite circular polarizations.

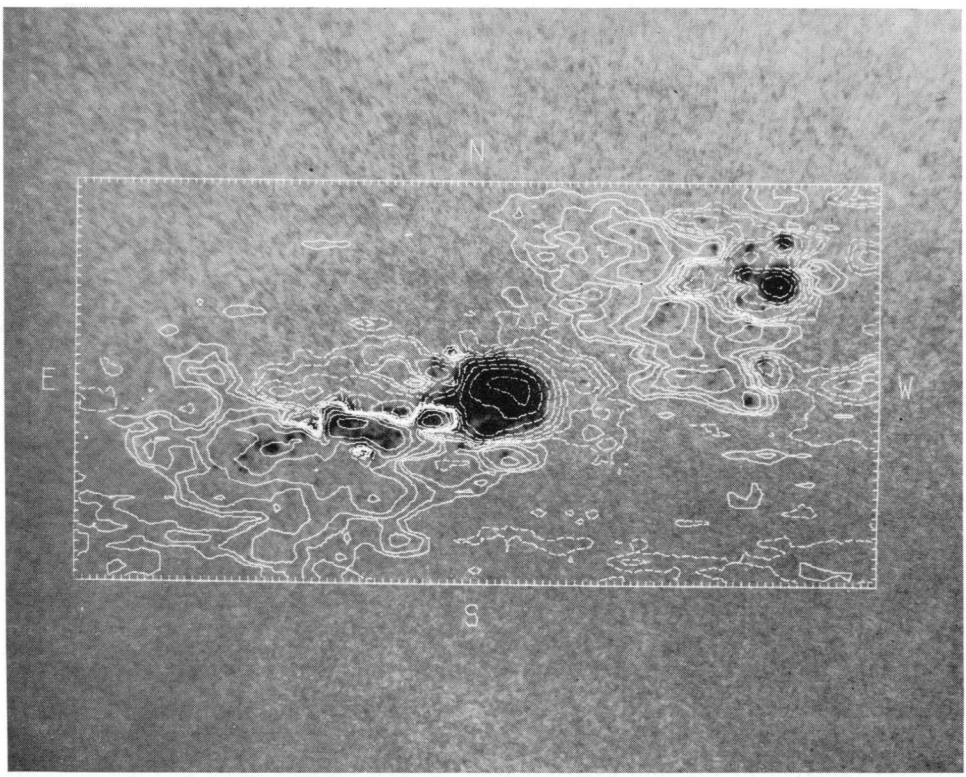

Fig. 3. Isogauss map as produced by digital recording and by computer reduction of the Sacramento Peak Magnetometer signal (courtesy D.M. Rust).

In the future we look forward to many refinements of the photoelectric magnetograph as for example the television and digital image tube applications being undertaken in Sydney, Aerospace and Huntsville. We could also start to make use of the fact that the Zeeman splitting varies as the square of the wavelength so that the effect of the fields are very much larger in the infrared.

In the near infrared ($\sim 2\mu$) there are a number of photospheric lines with large Zeeman splitting which might profitably be used. The disadvantage in this wavelength region is of course the poor performance of the detectors. Fourier spectroscopy is of

https://doi.org/10.1017/S0074180900022336 Published online by Cambridge University Press

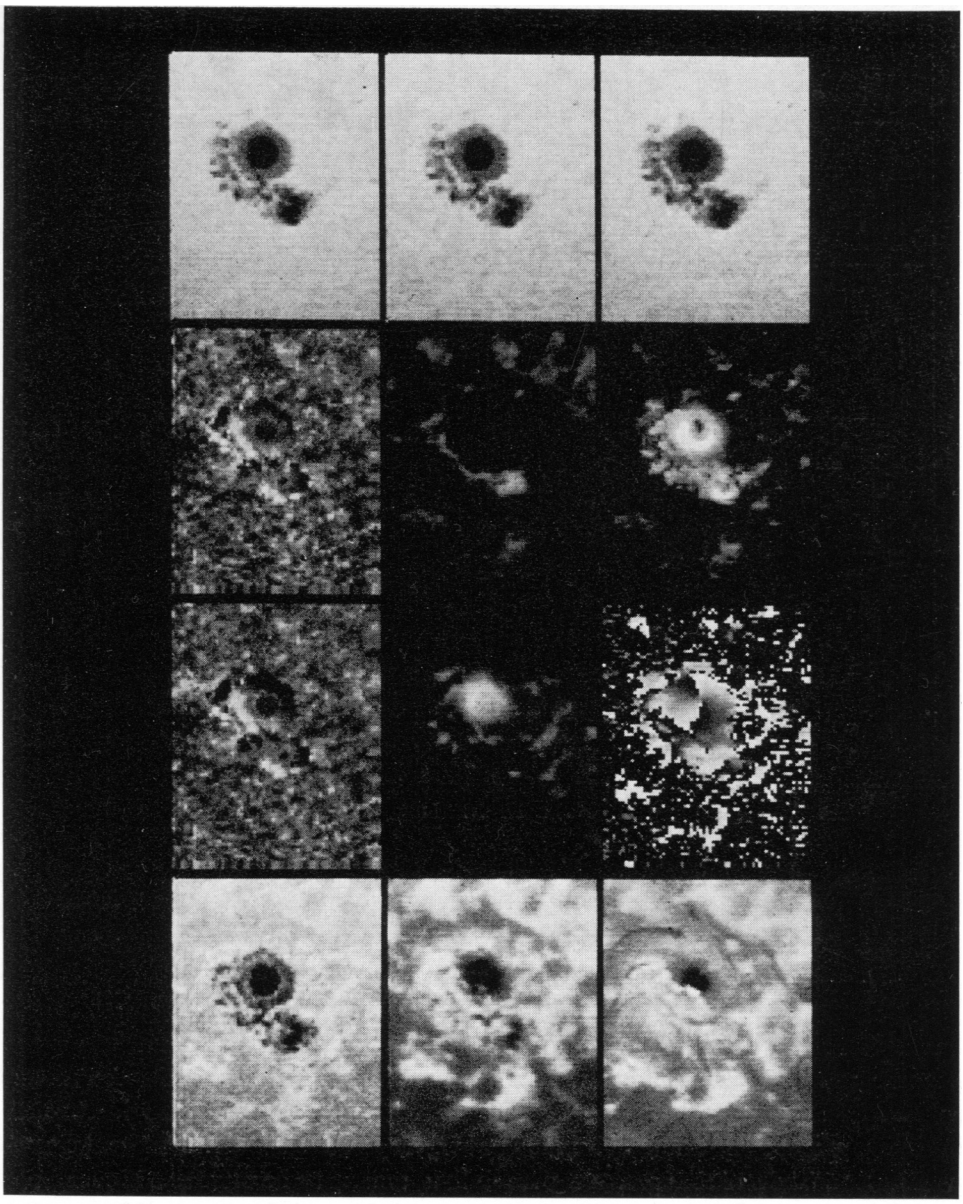

Fig. 4. Example of a display generated by computer of the Kitt Peak vector magnetograph signals. From left to right, top to bottom, the twelve displays represent: (1) the continuum intensity, (2) the wing brightness of λ5233, (3) the wing brightness of λ5250, (4) the Doppler velocity in λ5233, (5) the positive longitudinal field, (6) the strength of the transverse field, (7) the Doppler velocity in λ5250, (8) the negative longitudinal field, (9) the direction of the transverse field, (10) the brightness in the core of λ5250, (11) the K232 brightness, and (12) the Hα brightness (courtesy W. Livingston and J. Harvey).

https://doi.org/10.1017/S0074180900022336 Published online by Cambridge University Press

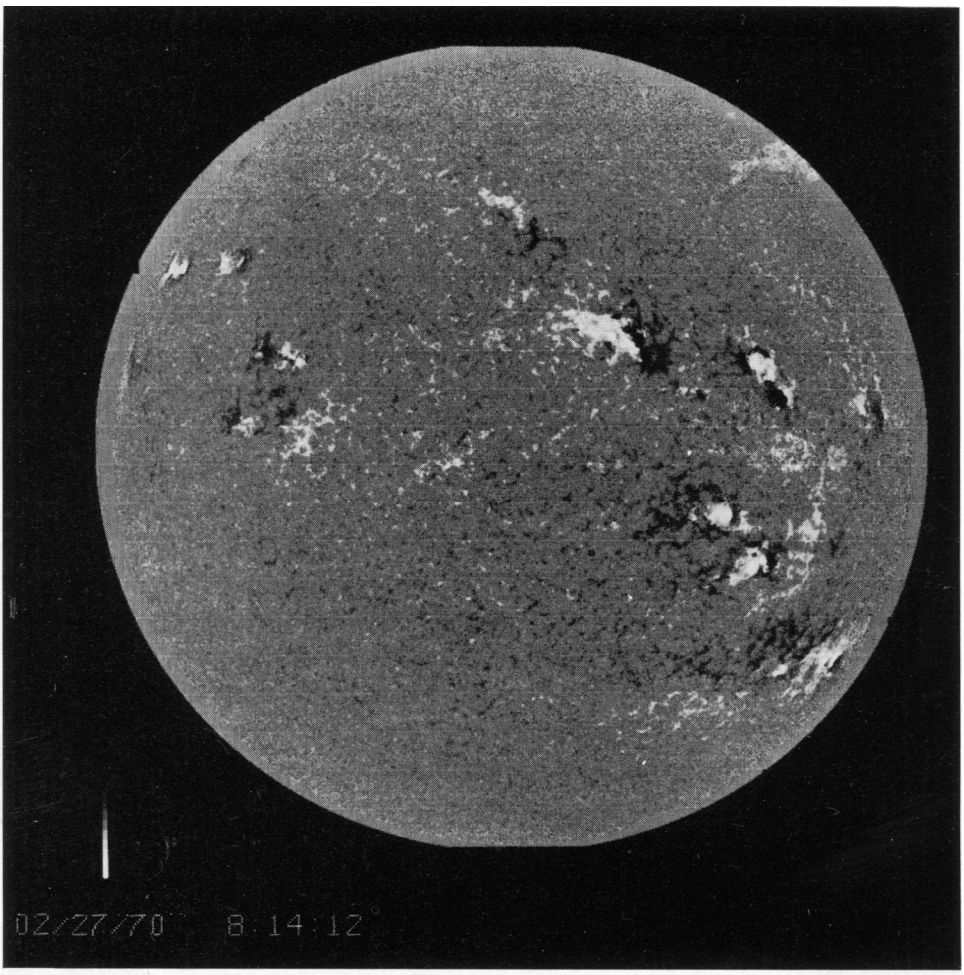

Fig. 5. Example of a display generated by computer of the longitudinal magnetic field as measured with the 40 channel Kitt Peak magnetograph (courtesy W. Livingston, J. Harvey and C. Slaughter).

little help since the magnetograph uses only one or two distinct wavelengths. One might exploit however the possibility of making a spatial Fourier analysis along the spectrograph slit. This should give the same signal to noise ratio multiplex advantage as Fourier analysis of the spectrum gives so that it might be possible to achieve a good sensitivity. Spatial Fourier analysis can for example be made by means of Savart plate interferometers presently used to study modulation transfer functions (Steel (1969)) or by some direct mechanical device.

In the extreme infrared or microwave region Dupree (1968) predicted the existence of recombination lines originating in high levels of hydrogenic coronal ions. These lines are very numerous at wavelengths longer than 700μ which can only be observed from high altitude stations. Their Landé factor is about one resulting in a Zeeman

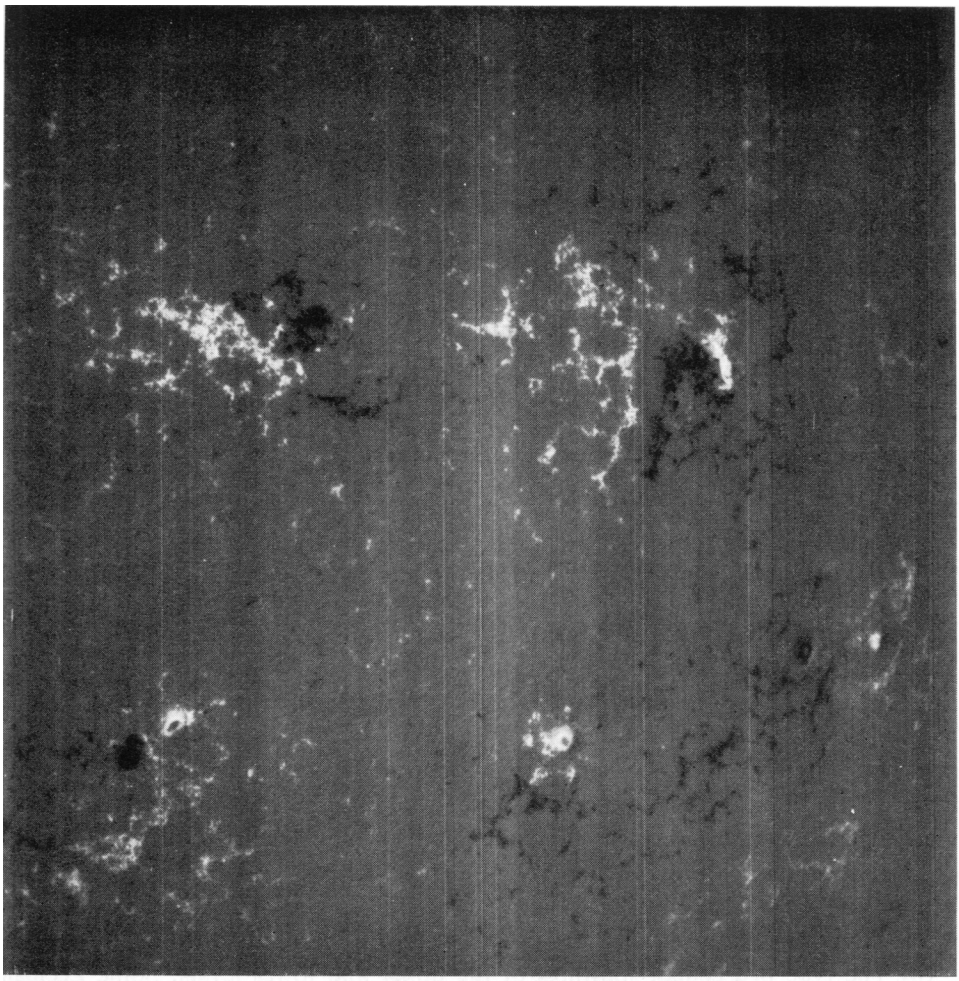

Fig. 6. Magnetogram obtained by photographic subtraction (Leighton's method) (courtesy D. Vrabec, Aerospace Corporation).

splitting of 0.08 μ, which equals the thermal Doppler width of the line ($T = 2 \times 10^6$ K), for only 17 G for a line at 1 mm. This could become a very powerful tool for studying coronal magnetic fields after the existence of these lines has been confirmed. It may be that in this case the observation can best be done by Fourier spectroscopy. It is in this context of interest therefore to describe the Fourier Transform of a Zeeman split line. If $P(s)$ equals the Fourier transform of $p(\lambda)$ such that

$$P(s) = \int_{-\infty}^{+\infty} p(\lambda)\, e^{-2\pi i s\lambda}\, \mathrm{d}\lambda \tag{4}$$

it follows from Equations (1) that the Fourier transforms $\{P_I, P_Q, P_U, P_V\}$ of the four

https://doi.org/10.1017/S0074180900022336 Published online by Cambridge University Press

Stokes parameters are:

$$P_I(s) = [\cos^2(\pi s \Delta\lambda_B) - \cos^2\gamma \sin^2(\pi s \Delta\lambda_B)]\, P(s) \approx P(s) \tag{5}$$

$$P_Q(s) = \sin^2\gamma \sin^2(\pi s \Delta\lambda_B)\, P(s) \approx \pi^2 s^2 \Delta\lambda_B^2 \sin^2\gamma P(s) \quad (:)\ B_\perp^2 \tag{5'}$$

$$P_U(s) = 0 \tag{5''}$$

$$P_V(s) = i \cos\gamma \sin(2\pi s \Delta\lambda_B)\, P(s) \approx 2\pi i s \Delta\lambda_B \cos\gamma P(s) \quad (:)\ B_\parallel . \tag{5'''}$$

Where the $\approx$ signs refer to small $\Delta\lambda_B$. The P_Q and P_V becomes zero for $s = \frac{1}{2}\Delta\lambda_B$ and $s = 1/\Delta\lambda_B$ respectively so that $\Delta\lambda_B$ or $|B|$ can be determined much more easily from the P_Q and P_V profiles than from the Q or V profiles. For small $\Delta\lambda_B$ this zero point moves towards infinity and becomes hard to determine because of the small amplitude of $P(s)$. Then the P_Q and P_V contain only information on $B_\perp^2$ and $B_\parallel$ respectively.

2.2. The Hanle effect

Observations of prominences and of the corona outside the solar limb show that the emission lines often have a significant amount of linear polarization with the direction of polarization making some rather arbitrary angle with respect to the solar limb. This polarization is due to the so-called Hanle effect. The Hanle effect refers to the resonance scattering of bound electrons in the presence of a magnetic field (Mitchell and Zemansky (1961)). For a zero magnetic field and for electric dipole transitions this scattering results in linear polarization with the dominant electric vector parallel to the limb. For weak fields the excited electron gyroprecesses in the field so that the direction of polarization of the emitted radiation, as well as the degree of polarization, is changed. The degree and direction of linear polarization is therefore a function of the magnetic field. In addition to being related to the field the polarization is also dependent on the following factors:

(a) The ratio of collisional to radiative excitations. The fraction of the excitations which are collisional does of course not give rise to polarized emission.

(b) The type of Zeeman splittings of the upper and lower levels. Some Zeeman splittings (e.g. $J=1$ upper level, $J=0$ lower level) give a maximum polarization (100% for zero field and extreme anisotropic radiation field). Others (e.g. $J=0$ for upper level, $J=1$ for lower level) give always zero polarization.

(c) The ratio δ of Larmor frequency $\omega_L = eB/m_e c$ to the damping constant of the excited state. This determines the amount the electron can gyroprecess before emitting. Generally this damping constant is taken equal to the radiative damping constant. For dense media the collisional damping constant has to be taken into account also.

(d) The properties of the incident radiation field.

(e) The optical thickness of the object under study. Multiple scattering may become significant for large thicknesses.

(f) The interlocking with other atomic levels and other radiation transfer phenomena like frequency dependent source functions.

If all of these effects are known and taken into account one can calculate, for a known field, the polarization due to the Hanle effect. This has been done to various

degrees of completeness for example by Hyder (1964) and House (1970). Figure 7 shows some of the results obtained by House. In Figure 7 the degree p_{max} and the angle α'_{max} of linear polarization is shown for a $J_{upper}=1$ and $J_{lower}=0$ transition like the Ca I λ4227 line or the Fe XIII λ10747 line. The magnetic field vector lies in a plane parallel to the solar limb and makes an angle θ' with the direction to the line of sight. The quantity Δ is directly proportional to the magnetic field. It is equal to 1 for 70G in the permitted λ4227 line and 0.3 microgauss in the forbidden λ10747 line. For zero

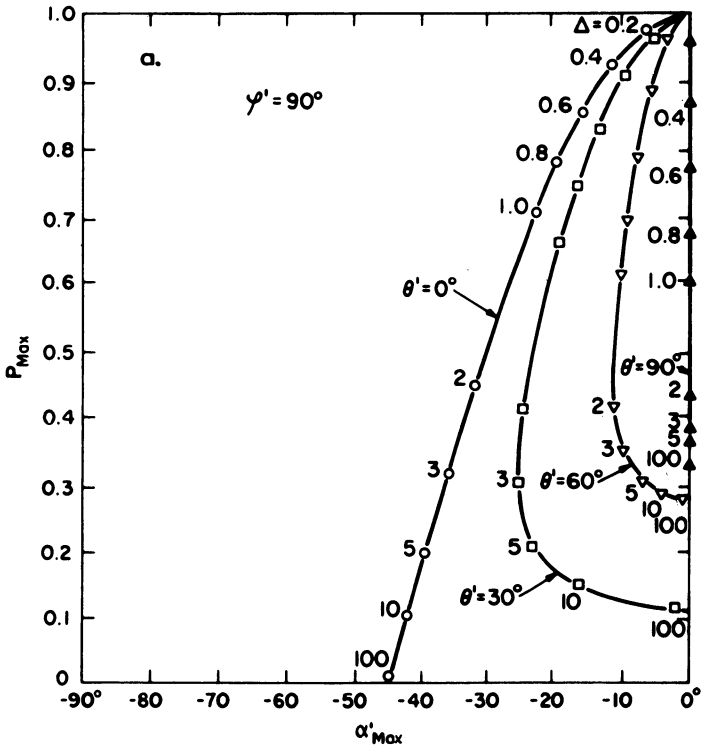

Fig. 7. Degree p_{max} and direction α'_{max} of linear polarization of a $J_{lower}=0$ and $J_{upper}=1$ line (e.g. λ4227). Illumination is unidirectional at right angle to the line of sight. The magnetic field vector lies in the plane at right angles to the illumination direction and makes an angle θ' with the line of sight. Δ is a measure of the field strength (see text). The collisional excitations and multiple scattering have been neglected (courtesy L. House).

field one has maximum polarization at $\alpha'=0$ or parallel to the limb for the permitted electric dipole radiation like λ4227 and at right angles to the limb for the forbidden magnetic dipole radiation like λ10747. With increasing field strength the amount of polarization decreases and the direction changes. There is no simple relationship between the amount and direction of linear polarization and the strength and direction of the magnetic field. Only with very large approximation can one say that the degree of polarization is related to the total field strength and the direction to the longitudinal magnetic field strength.

https://doi.org/10.1017/S0074180900022336 Published online by Cambridge University Press

Apart from the Hanle effect there are two other effects which may give rise to linear polarization. These are (a) the transverse Zeeman effect, and (b) the so-called impact polarization resulting from collisional excitation by anisotropic particle (electron) streams as occur during solar flares. Generally these two effects can be neglected.

The Hanle effect has been used for magnetic field determinations in prominences (e.g. Hyder, 1964, 1965, 1966; Brückner, 1966; Nikolskii *et al.*, 1970) and in the corona (e.g. Hyder, 1965; Charvin, 1965). It may also complicate transverse magnetic field observations on the solar disk by Zeeman magnetographs as discussed by Hyder (1968) and Lamb (1970).

2.3. The gyro-synchrotron radiation

Free electrons spiraling in a magnetic field also emit electromagnetic radiation whose frequency is directly related to the Larmor, or gyro frequency, $\omega_L = eB/m_e c = 1.76 \times 10^7 B \sec^{-1}$. For electrons with small kinetic energy the radiation occurs only at ω_L. This so called gyro-resonance radiation or magneto bremsstrahlung is strongest and circularly polarized in the so-called extraordinary mode when viewed along the field lines. Since on the Sun $B < 3000$ G this radiation occurs at frequencies < 10 GHz or at wavelengths > 3 cm so that the upper chromosphere and corona are the regions accessible by this phenomenon. When the electron velocities are no longer small but still not relativistic, and this is the case for thermal electrons in the quiet solar corona ($v/c \approx 0.02$) and for some radio bursts, radiation occurs also at the lower harmonics of the gyro frequency. For relativistic electrons, the gyro-resonance radiation turns into synchrotron radiation. In the synchrotron radiation the emitted energy is concentrated mainly in the plane of gyration, it has a very wide continuum-like spectral distribution, and it is polarized in this plane of gyration. Very good descriptions of these types of radiation are given by Takakura (1967).

The gyro-synchrotron radiation is strongly modified by propagation effects before it reaches the Earth. These are both absorption and refraction effects. Absorption is the inverse of the emission process just described. It is most efficient when the emission is most efficient and it is therefore much stronger for the extraordinary mode of circular polarization than for the ordinary. The magnetic field generally decreases with increasing height in the solar atmosphere so that the Larmor frequency decreases. The gyro-absorption occurs therefore at lower frequencies than the gyro-emission so that this effect tends to suppress the observed emission at low frequencies. Because it absorbs the extraordinary mode of polarization it may also make the polarization of the transmitted radiation ordinary. Refractive effects also prohibit the extraordinary ray at the gyro-frequency to escape. Only the higher harmonics in the extraordinary mode can therefore escape. The ordinary mode on the other hand can escape unhindered at the gyro frequency.

These absorption and refraction effects make the interpretation of the radio emission observations very difficult. Radiative transfer theories have been given by Kawabata (1954) and Kai (1965). These theories permit a fairly good derivation of the observable radiation for a given magnetic field configuration and a given thermal and non-

thermal electron distribution. To derive the magnetic field from the observation is however very difficult also because the observations are of low spatial resolution (worse than 1′) so that one probably averages over many different features. Nonetheless, many of the direct magnetic field measurements in the solar corona have come from the interpretation of gyro-resonance and synchrotron radiation effects.

Microwave type IV bursts (IVμ) and impulsive microwave bursts with brightness temperatures of 10^9 K are the most likely candidates for gyro-synchrotron emission by non-thermal electrons. These bursts are partially circularly polarized in the ordinary mode at low frequencies (<1000 MHz) and in the extraordinary mode at high frequencies (>10000 MHz). The emission reaches a maximum at ≈ 2000 MHz. Takakura (1966, 1967) finds from a quantitative evaluation of the emission and absorption processes that this maximum for gyro-synchrotron radiation should occur at about four times the gyro frequency $f_H = \omega_L/2\pi = 2.8 \times B$ MHz which results in a field strength

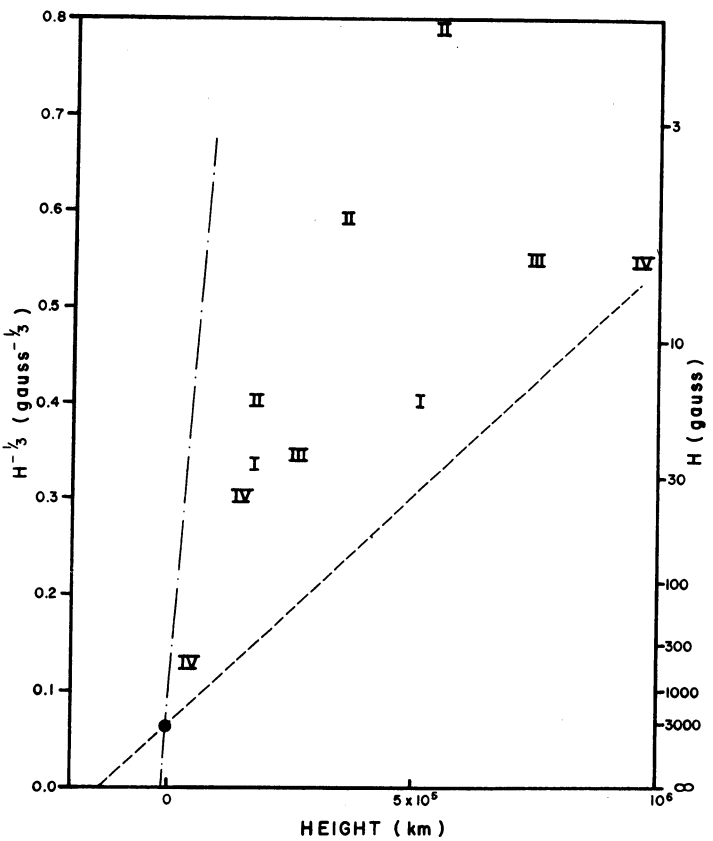

Fig. 8. Magnetic field determinations in the corona above sunspots as derived from radiobursts. The roman numeral indicates the type of burst. In the plot $B^{-1/3}$ to height a magnetic dipole represents a straight line. The dashed line represents the magnetic dipole distribution by Correll *et al.* (1956) from the paths of 'rain' type prominences near sunspots. The dash-dot line represents the dipole distribution determined by Ioshpa *et al.* from the magnetic field variation across the sunspot.

https://doi.org/10.1017/S0074180900022336 Published online by Cambridge University Press

of 200 G which is a reasonable value since the bursts occur ≈ 30000 km above sunspots. Similar arguments can be used to derive the field at greater heights from decimeter and meter type IV bursts (Figure 8). The interpretation of the polarization reversal is unclear. Takakura (1967) attributes it to a double source resulting from the bi-polar character of sunspots groups the preceding dominant spot giving the extraordinary mode at high frequencies and the following, weaker spot giving the ordinary mode at low frequencies. Earlier Takakura (1960) interpreted it as a single source phenomenon with the ordinary low frequency polarization caused by gyro-absorption. The latter interpretation results in a polarization reversal at 2–3 f_H which gives magnetic fields in agreement with the ones determined from the emission maximum.

Type I bursts, or the so-called noise storms, present a different example of magnetic field determination (Takakura, 1966). Their emission is thought to be due to plasma waves, their very high degree of circular polarization in the ordinary mode is interpreted as due to the inability of the extraordinary ray to escape because of refraction effects. This condition gives at the source of the plasma waves magnetic fields which are in agreement with those derived from the type IV bursts (Figure 8).

An example of gyro-resonance radiation from thermal electrons can be found in the radio emission occurring above sunspot umbrae. The properties of this emission have been discussed by Livshits *et al.* (1967). The brightness temperature of sunspot *e* mounts to as much as 10^6 in the cm wavelength region, the radiation being polarized in the extraordinary mode. Livshits *et al.* derive a temperature model of the sunspots chromosphere and corona from these data with an assumed magnetic field distribution and a hydrostatic density profile.

2.4. The Faraday Rotation

The amount of Faraday rotation is given by

$$\phi = 2.36 \times 10^{-3} f_{\mathrm{MHz}}^{-2} \int N_e B_z \, \mathrm{d}_z$$

where the integral is taken over the path between source and observer and where B_z equals the longitudinal magnetic field. In principle it is therefore possible to estimate B_z if the amount of Faraday rotation is known. The latter can be derived for example from the frequency dependence of ϕ. The amount of rotation is however so large that ϕ changes significantly within the bandwidth so that the linear polarization of the source is lost. The requirements to observe the Faraday rotation therefore are: (a) a linearly polarized source. This could be, for example, a synchrotron radiation source or also a linearly polarized radar signal. (b) Narrow bandwidth so that the rapid frequency variation of ϕ can be studied (Akabane *et al.*, 1961). The Faraday effect as a means of magnetic field determination in the solar corona has been used very little. Golnev *et al.* (1964) determined an upper limit to the field of 10^{-2} G at $5 R_\odot$ by using the Crab Nebula as the source of linear polarization while Bhonsle *et al.* (1964) determined relative values of the coronal field from a type III burst source.

3. Magnetic Fields as Studied by their Influence on the Solar Atmosphere

In the regions of the solar atmosphere where the magnetic pressure $P_B = B^2/8\pi$ exceeds the gas or kinetic pressure (resp. P_g and $P_k = \frac{1}{2}\varrho v^2$) one expects a strong influence of the magnetic field on the physical conditions. Such regions are: parts of the photosphere such as sunspots, pores and faculae, all of the chromosphere and all of the corona except the solar wind. From the study of the physical conditions of these regions it is therefore often possible to infer some of the properties of the magnetic field.

Fig. 9. Hα filtergram of an active region (courtesy R. B. Dunn).

https://doi.org/10.1017/S0074180900022336 Published online by Cambridge University Press

3.1. The alignment of structures

Plasma motions generally follow magnetic field lines so that there tends to be an alignment of matter in the solar atmosphere which coincides with the direction of the magnetic field. The study of these alignments is, in my opinion, by far the best way of determining the projected direction or azimuth of the field lines. In this way one can determine the field direction in sunspot penumbrae from white light photography, and in the chromosphere from spectroheliograms. In the corona one can use limb observations made during an eclipse or with a coronagraph and disk observations made with high resolution X-ray telescopes. Also to be included in this category of measuring magnetic fields are the directions of the filamentary structures in the outer corona as inferred from the observation of anisotropic scattering of the crab nebula radio radiation. Figure 9 shows as an example an Hα filtergram of a sunspot region. Here, as in quiet regions, the alignment of the fibrils and elongated fine mottles shows the structure of the magnetic field in such detail as is virtually impossible to obtain by transverse magnetographs.

3.2. Local changes in the atmosphere model

When $P_B > P_g$ one expects significant changes of the temperature and density structure of the solar atmosphere. In the photosphere this condition occurs in sunspots and pores; wherever we see such a structure we are therefore sure that we also see a region with a magnetic field >1500 G. Because of the much lower densities, this condition holds over almost all of the chromosphere and the corona and over much of the upper photosphere. Figure 10 shows as example a spectroheliogram in the CN bands at 3888 Å. Chapman and Sheeley (1968) find that these CN brightness structures in the upper photosphere coincide with magnetic fields of the order of 300 G. The same has been shown to be the case for the chromospheric H and K line network except that there the brightening occurs at weaker fields. We do not know yet however whether the amount of brightening is uniquely related to the absolute field strength, to the vertical field strength or to some other parameter related to the field. We also cannot determine the direction of the field, although, together with the alignment information, one can take a good guess at this.

3.3. The propagation of rapid disturbances

One often sees disturbances propagate with velocities greater than the sound velocities. One of the explanations for these high velocities is that the disturbance is of a magneto-hydrodynamic type which propagates with the Alfvén speed $V_A = B/\sqrt{4\pi\varrho}$. Such explanations have been made plausible in a number of cases which therefore have resulted in an estimate of B. Takakura (1966) derives in this way the magnetic fields above a sunspot from the propagation in frequency, and therefore in height, of type II bursts (see Figure 8). Meyer (1968) inferred in this way from the propagation of the Moreton waves an average coronal magnetic field of 6 G.

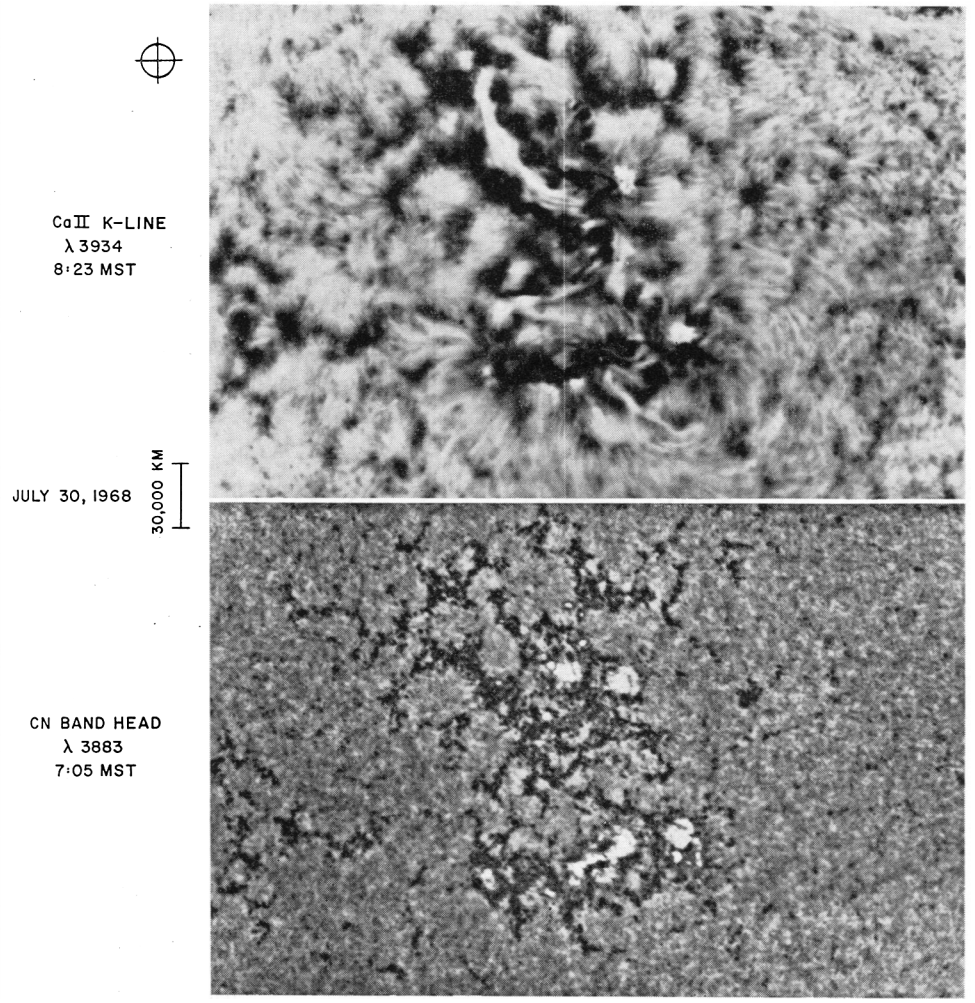

Fig. 10. Spectroheliograms taken in the K line and in the CN bandhead. The latter shows the bright 'photospheric' network which coincides with the photospheric magnetic field structure (courtesy N. R. Sheeley, Jr.).

3.4. Oscillations of prominences

After large flares filaments up to 40° away are occasionally seen to have a velocity oscillation which manifests itself in Doppler shift oscillations in the Hα line. Hyder (1966) and Kleczek *et al.* (1969) explain this phenomenon by introducing a restoring force resulting from the magnetic tension. The difference between the two investigations results from the interpretation of the oscillation to be respectively vertical or horizontal. This results in a difference in the interpretation of the damping mechanism of the oscillation. The period of oscillations in both cases comes out within the same order of magnitude. However, it is related to the magnetic field by: $B=4\pi \mathrm{H} f \sqrt{\pi \varrho}$ where

https://doi.org/10.1017/S0074180900022336 Published online by Cambridge University Press

H=height of the filament ($\approx 3 \times 10^4$ km) and f= the frequency of oscillation ($\approx 10^{-3}$ s^{-1}). This results in a field strength of about 10G which is indeed consistent with measurements made using the Zeeman and Hanle effects.

4. Magnetic Fields as Inferred from Theoretical Consideration

There are some ways in which the magnetic field on the sun can be inferred from purely theoretical arguments.

4.1. Potential or current free field calculations

These calculations take the measurements of the longitudinal photospheric magnetic field as determined with Zeeman magnetographs. The assumption that there are no electric currents above the photosphere, or that curl $\mathbf{B}=0$ gives then the magnetic

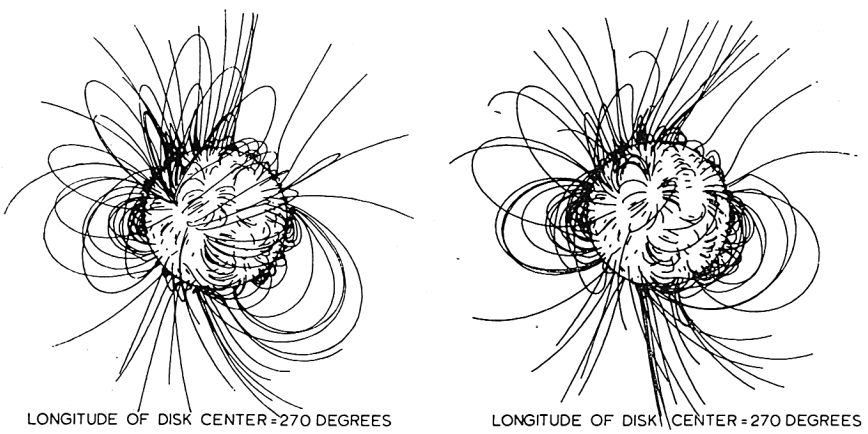

Fig. 11. Magnetic field distribution in the corona as determined from the potential field assumption (courtesy M. D. Altschuler and G. A. Newkirk).

field configuration in the corona. The general solution of this potential field approximation in spherical coordinates has been given by Altschuler *et al.* (1969). It uses an expansion of the magnetic potential in Legendre polynomials, the coefficients of this expansion being determined by a least squares fitting of the observed longitudinal photospheric magnetic field. Figure 11 gives an example of the field configuration in the corona obtained in this way. A refinement of the method permits the inclusion of the solar wind so that the field lines in the outer corona are made approximately radial.

4.2. Equipartition of magnetic and kinetic energies

In a convective medium magnetic fields tend to be concentrated towards the edges of the convection cells. According to Weiss (1966) it takes typically 3 turnover times to reach the maximum field strength whose magnitude is such that the kinetic and magnetic energy densities are comparable although the latter can never exceed the former.

For the supergranulation one derives in this way magnetic fields which are of the same magnitude as have been observed (Parker, 1963; Clark *et al.*, 1967). For the solar core this procedure gives magnetic fields of the order of 10^9 G and for the deep convective zone 10^5 G.

5. Conclusion

In Table II, I summarize the methods which can be used to determine the magnetic fields in the various zones on the Sun. Each of these methods has its own merits which makes it occasionally preferable over the other methods. None of the methods permits as yet an accurate determination of the complete field vector. The closest to this comes the Zeeman Vector Magnetograph. It can however only be used well in the solar photosphere. The interpretation of its signals in terms of the magnetic field vector is sufficiently complex and difficult that a reliability of a factor of 2 seems almost optimistic.

The magnetic field is however one of the, if not *the*, most important physical quantity in the observable solar atmosphere. Its measurement by any available method is therefore of the greatest importance. By future refinements of the measurements and their interpretation, by improvements in the theories of the solar radiation in the presence of a magnetic field and by exploring new ways in which to measure magnetic fields we may therefore expect to significantly improve our understanding of the physics of the solar atmosphere.

TABLE II

Summary of ways of measuring solar magnetic fields

Effect		Region on the Sun			
		Int.	Phot.	Chrom.	Cor.
Electromagnetic radiation					
Zeeman Effect	Visual		X	X	(X)
	Near IR ($\sim 2\mu$)		X	X	(X)
	Far IR ($\sim 700\mu$)				X
	UV			X	X
Hanle Effect (Hα, D_3, etc., Lyman α?)				X	X
Gyro-Synchrotron radiation (radio)					X
Faraday rotation					X
MHD Effects					
Alignments of structures (Hα, Corona, penumbral filaments)			(X)	X	X
Influence on T, P structure (K-brightness CN network)			(X)	X	X
Alfvén velocity $V_A = B/\sqrt{4\pi\varrho}$				X	X
Prominence Oscillations					X
Theory					
$P_g \approx P_B$		(X)	(X)		
Force free/Potential field				X	X

https://doi.org/10.1017/S0074180900022336 Published online by Cambridge University Press

References

Akabane, K. and Cohen, M. H.: 1961, *Astrophys. J.* **133**, 258.
Altschuler, M. D. and Newkirk, G.: 1969, *Solar Phys.* **9**, 131.
Athay, R. G.: 1970, *Solar Phys.* **12**, 175.
Babcock, H. W.: 1953, *Astrophys. J.* **118**, 387.
Beckers, J. M.: 1968a, *Solar Phys.* **3**, 367.
Beckers, J. M.: 1968b, *Solar Phys.* **5**, 15.
Beckers, J. M.: 1969, AFCRL-Physical Sciences Research Papers, No. 371.
Beckers, J. M. and Schröter, E. H.: 1969, *Solar Phys.* **10**, 384.
Beggs, D. W. and Von Klüber, H.: 1969, *Monthly Notices Roy. Astron. Soc.* **127**, 133.
Bhonsle, R. V. and McNarry, L. R.: 1969, *Astrophys. J.* **139**, 1312.
Brückner, G.: 1966, in *Atti del Convegno sui Campi Magnetici Solari* (ed. by M. Cimino), G. Barbèra, Firenze, p.101.
Chapman, G. A. and Sheeley, N. R.: 1968, *Solar Phys.* **5**, 442.
Charvin, P.: 1965, *Ann. Astrophys.* **28**, 877.
Clark, A. and Johnson, H. K.: 1967, *Solar Phys.* **2**, 433.
Correll, M., Hazen, M., and Bahng, J.: 1956, *Astrophys. J.* **124**, 597.
Deubner, F. L. and Liedler, R.: 1969, *Solar Phys.* **7**, 87.
Dupree, A. L.: 1969, *Astrophys. J.* **152**, L125; and Thesis, Harvard Univ., 1968.
Evans, J. W.: 1966 in *Atti del Convegno sui Campi Magnetici Solari* (ed. by M. Cimino), G. Barbèra, Firenze, p.123.
Golnev, V. J., Parijsky, Y. N., and Soboleva, N. S.: 1969, *Izv. Pulk. Obs.* **23**, 22.
Harvey, J. and Livingston, W.: 1969, *Solar Phys.* **10**, 283.
House, L. L.: *J. Quant. Spectr. Radiative Transfer*, submitted 1970.
Hyder, C. L.: 1964, Thesis, University of Colorado.
Hyder, C. L.: 1965a, *Astrophys. J.* **141**, 1374.
Hyder, C. L., 1965b, *Astrophys. J.* **141**, 1382.
Hyder, C. L.: 1966, *Z. Astrophys.* **63**, 78.
Hyder, C. L.: 1968, *Solar Phys.* **5**, 29.
Hyder, C. L.: 1969, in *Atti del Convegno sui Campi Magnetici Solari* (ed. by M. Cimino), G. Barbèra, Firenze, p.110.
Ioshpa, B. A. and Obridko, V. N.: 1964, *Geomagnetism Aeronomy* (Engl. ed.) **4**, 12.
Ioshpa, B. A. and Obridko, V. N.: 1965, *Soln. Aktivnost* **2**, 131.
Ioshpa, B. A. and Obridko, V. N.: 1965, *Soln. Dann.* **3**, 54.
Kai, K.: 1965, *Publ. Astron. Soc. Japan* **17**, 309.
Kawabata, K.: 1964, *Publ. Astron. Soc. Japan* **16**, 30.
Kleczek, J. and Kuperus, M.: 1969, *Solar Phys.* **6**, 72.
Kuznetzov, D. A., Kuklin, G. V., and Stepanov, V. E.: 1966, *Results IQSY* **1**, 80.
Lamb, F. K.: 1970, *Solar Phys.* **12**, 186.
Lee, R. H., Rust, D. M. and Zirin, H.: 1965, *Appl. Opt.* **4**, 1081.
Livingston, W. and Harvey, J.: 1970, Preprint.
Livshits, M. A., Obridko, V. N., Pikel'ner, S. P.: 1967, *Soviet Astron.* **10**, 909.
Meyer, F.: 1968, in K. O. Kiepenheuer (ed.), 'Structure and Development of Solar Active Regions', *IAU Symp.* **35**, 485.
Mitchell, A. G. and Zemansky, M. W.: 1961, *Resonance Radiation and Excited Atoms*, Cambridge University Press, 2d Ed.
Nikolskii, G. M. and Kretsuriani, Ts. S.: 1970, *Soviet Astron.* **13**, 815.
Parker, E.: 1963, *Astrophys. J.* **138**, 552.
Rayrole, J.: 1967, *Ann. Astrophys.* **30**, 257.
Seares, F. H.: 1913, *Astrophys. J.* **38**, 99.
Severny, A. B.: 1967, *Izv. Krymsk. Astrofiz. Obs.* **36**, 22.
Steel, W.: 1964, *Opt. Acta* **11**, 9.
Stepanov, V. E. and Severny, A. B.: 1962, *Izv. Krymsk. Astrofiz. Obs.* **28**, 166.
Takakura, T.: 1960, *Publ. Astron. Soc. Japan* **12**, 325, 352.
Takakura, T.: 1966, *Space Sci. Rev.* **5**, 80.
Takakura, T.: 1967, *Solar Phys.* **1**, 304.

Weiss, N.: 1966, in *Atti del Convegno sui Campi Magnetici Solari* (ed. by M. Cimino), G. Barbèra, Firenze, p.299.
Wiehr, E.: 1969, *Solar Phys.* **9**, 225.
Zhulin, I. A., Ioshpa, B. A., and Mogilevsky, E. I.: 1962, *Geomagnetism Aeronomy* (Engl. ed.) **2**, 489.

Discussion

Semel: Are the given expressions for the Fourier transforms of the Stokes parameters valid for any model?

Beckers: The expressions refer to the Seares approximation for a Zeeman triplet. The detailed theory of line formation to be discussed by Dr. Stenflo tomorrow will be able to give the Fourier transforms for more general cases. The properties of the Fourier Stokes Parameters will be similar, however, to those discussed for the Seares approximation.

Maltby: In connection with the Zeeman measurements could you comment on the use of electro-optical polarization optics as compared to rotation of polarization optics. By rotating a linear polarizer at a much higher speed than the rotation frequency of a quarter wave plate all 4 Stokes parameters may be determined. Will the rotating system be too slow?

Beckers: There are two disadvantages in using rotating polarization optics: (1) The speed of rotation can generally not be made very high. This results in modulation frequencies which fall in the range of the frequencies associated with the atmospheric seeing. The seeing becomes in this case a serious source of noise. This is not the case for electro-optical devices which can be operated in the kilohertz range (2) Rotation of optics causes slight changes in the optical paths (dust, motion of light on photocathode etc.) resulting in spurious signals.

Foukal: Which infra-red lines around 2 microns do you consider best suited to Zeeman effect measurements?

Beckers: Dr. Hall has a list of these lines. I remember specifically a Titanium line at $2.3\,\mu$.

Simon, M.: I would like to add that there is another effect which may be used at radio wavelengths in addition to those discussed by Dr. Beckers. This is the suppression of gyro-synchrotron radiation in the presence of a plasma - the Razin effect. It results in a sharp low frequency cut-off, and was first observed in a moving Type IV burst by Boischot and his co-workers. The burst was analyzed by them, Ramaty, and also Bohlin and myself. Bohlin and I determined the field in the streamer in which the burst took place to be $\sim\frac{1}{4}$ G at a height $\sim 1\,R_{\odot}$.

Beckers: This effect should indeed be added to my list.

Pasachoff: Pulsars are also sources of both circularly and linearly polarized radiation behind the solar corona, and so those that are occulted could conceivably be used as probes for Faraday rotation measurement, although the solar contribution is small. Frequency dispersions of pulses from pulsars is already being used to assess electron densities in the outer corona. Care must be taken to calibrate the polarization in different parts of the pulses.

For all rotation studies, one must independently monitor the considerable rotation introduced by the Earth's ionosphere. This contribution varies both rapidly and diurnally by large factors.

Beckers: This is indeed another possibility.

Brueckner: When extrapolation of measured photospheric fields into the chromosphere are made, the assumption of current-free fields is made from a certain altitude. At which optical depth is this assumption allowed?

Beckers: We do not know yet. There are conflicting opinions on whether the field above the photosphere, where the Zeeman magnetograph measurements are made, is current free.